A Function-Based Maximum Power Point Tracking Method for Photovoltaic Systems

S. M. Reza Tousi, *Member, IEEE*, Mohammad Hassan Moradi, *Member, IEEE*, Nasser Saadat Basir, and Milad Nemati

***Abstract*—In this paper, a novel maximum power point tracking (MPPT) algorithm based on introducing a complex function for photovoltaic (PV) systems is proposed. This function is used for determination of the duty cycle of the dc–dc converter in PV systems to track the MPP in any environment and load condition. It has been suggested based on analyzing the expected behavior of converter controller. The function is formed by a two-dimensional Gaussian function and an Arctangent function. It has been shown that contrary to many algorithms that produce wrong duty cycles in abrupt irradiance changes, the proposed algorithm is able to behave correctly in these situations. In order to evaluate the performance of method, various simulations and experimental tests have been carried out. The method has been compared with some major MPPT techniques with regard to start-up, steady-state, and dynamic performance. The results reveal that the proposed method can effectively improve the dynamic performance and steady-state performance simultaneously.**

***Index Terms*—Gaussian–Arctangent function-based MPPT, maximum power point tracking (MPPT), photovoltaic (PV) systems, variable perturbation frequency.**

I. Introduction

MAXIMUM power point tracking (MPPT) is one of the major concerns in photovoltaic (PV) systems and plays a vital role in utilization of these systems for practical applications. Each PV cell has a special point named maximum power point (MPP) on its operational curve (i.e., current–voltage or power–voltage curve) in which it can produce maximum possible power. These operational curves change nonlinearly with changes in irradiance and temperature of environment. So, the nonlinear dependency of MPP on environment parameters has led to development of various MPPT algorithms. These algorithms differ from one another considering factors such as the amount of energy extracted from the PV panel [tracking factor (TF)] [1], dynamic response, complexity, adaptation to environment changes, sensor requirements, and cost of implementation.

One of the first yet straightforward methods in the field of MPPT is perturbation and observation (P&O) method [2]. It is also the most prevalent MPPT method in industry applications because of its reasonable balance between simplicity and performance. In spite of its simplicity, P&O suffers from some defects such as trapping in local minima, maloperation in case of abrupt irradiance change, and even incorrect identification of MPP direction in this situation [3], [4]. Slow dynamic response in case of small step sizes, low efficiency at large step sizes, and permanent oscillation around MPP are the other defects of P&O algorithm. The efforts toward resolving or alleviating aforementioned problems led to development of many methods [5]-[14]. Improved P&O method is one of them which changes the perturbation amplitude based on the slope of PV curve. Furthermore, recently some methods have been proposed based on utilizing a single current or voltage sensor on the load side. The load-current adaptive step size and perturbation frequency (LCASF) [15] is one of them, which adaptively generates variable perturbations with variable periods in order to achieve fast and stable dynamic response in transients and less oscillations in steady state. Although, variable perturbation has mitigated some issues, these methods are still unable to resolve the maloperation in case of intensive environment variations. In portable applications such as solar vehicles and military portable solar coats used for charging of communication instruments or inside regions in which the clouds are formed in myriad of pieces, the frequent and abrupt changes in irradiation make the application of efficient MPPT algorithms with fast and correct response a requisite. In case of using MPPT methods that perform wrong operations frequently, a lot of energy will definitely be lost during a day.

In this paper, a new MPPT algorithm has been proposed. The novelty of the method lies in introducing an analytical function for generating a correct and adaptive perturbation step size. The proposed function is able to exhibit all desired behaviors both in steady-state and transient situations. This type of methods can form a new group of function-based MPPT algorithms. In this research, the Gaussian–Arctangent function-based (GAF) MPPT with variable perturbation frequency has been introduced. The proposed method has been simulated in MATLAB/Simulink workspace and compared with some MPPT methods. The results reveal the efficiency of method in steady-state and dynamic tests. In order to validate the simulation results, the controller is realized by a digital controller and tested on a boost converter delivering power from a PV system.

II. Proposed MPPT Technique

A typical PV solar system consists of a PV panel, a dc–dc converter, the MPPT controller, and a load. In this study, a boost

Manuscript received November 16, 2014; revised March 1, 2015; accepted April 10, 2015. Date of publication April 27, 2015; date of current version November 16, 2015. Recommended for publication by Associate Editor C. A. Canesin.

S. M. Reza Tousi, M. H. Moradi, and M. Nemati are with the Department of Electrical Engineering, Faculty of Engineering, Bu-Ali Sina University 6517838695 Hamedan, Iran (e-mail: tousi@basu.ac.ir; mh_moradi@yahoo.co.uk; en.nemati@yahoo.com).

N. S. Basir was with the Department of Electrical Engineering, Faculty of Engineering, Bu-Ali Sina University, Hamedan, Iran. He is now with the Ferdowsi University 9177948974 Mashahd, Iran (e-mail: Nasser.basir@gmail.com).

Color versions of one or more of the figures in this paper are available online at http://ieeexplore.ieee.org.

Digital Object Identifier 10.1109/TPEL.2015.2426652

converter has been used. The other part of this system is load, which can be a battery or a resistive load. The MPPT controller is responsible for adjusting the duty cycle of the boost converter to reach the MPP of the PV panel. The necessary measurements in this method are current and voltage.

A. Description of Method

In this method, the inputs of MPPT controller are E and ΔE, which are defined by (1) and (2). These inputs are the same as the inputs of fuzzy MPPT method, as presented in [16]

$$E(n) = \frac{p(n) - p(n-1)}{V(n) - V(n-1)} \tag{1}$$

$$\Delta E(n) = E(n) - E(n-1) \tag{2}$$

where n is the sampling time, $p(n)$ is the instantaneous output power of PV panel, $V(n)$ is the instantaneous output voltage of PV panel corresponding to nth sample, E is the tracking error, and ΔE is the change in error. The sign of E indicates that the operating point is located in the left or right side of MPP on P–V curve, while $\Delta E(n)$ determines the direction of its movement. The first step of the algorithm is measurement of variables (current and voltage) and computation of algorithm inputs (E and ΔE). Hereinafter, there are two distinct issues that must be addressed in the design of controller, and they are determining the next duty cycle perturbation step size (ΔD) and its period or delay time (T_{Delay}). Each of these two control variables plays a different role in performance of MPPT algorithm.

1) Size of Perturbation: Proper selection of perturbation step size depends on making a tradeoff between the speed and accuracy of tracking [15]. While a large ΔD speeds up the convergence of the algorithm, a small ΔD limits the power loss and oscillations around MPP in steady state. As stated before, the novelty of this paper lies in introducing a method for generating an adaptive perturbation step size by an analytical function. The function uses E and ΔE for computation of next perturbation step size (ΔD)

$$\Delta D = f(E, \Delta E) \tag{3}$$

where the next step duty cycle is calculated by

$$D(n+1) = D(n) + \Delta D(n). \tag{4}$$

2) Frequency of Perturbation: The other important control variable in this method is the frequency of perturbation. When a controller applies a perturbation to the system, it takes a time to settle in the next operating point. If the perturbation period becomes lower than the settling time of the system response, the system is never allowed to reach a steady state and its response at a particular time is affected by previous perturbations resulting in chaos-like behavior [17]. The frequency of perturbation can be adapted with variable steps in two ways. The first method used in FXS P&O is calculation of perturbation frequency based on the worst case (i.e., the largest perturbation), but this leads to a slow dynamic response of system [18], [19]. In order to alleviate this problem, another method proposed in [15]. The method computes the delay time per iteration using a linear formula. In this research, the same method has been used

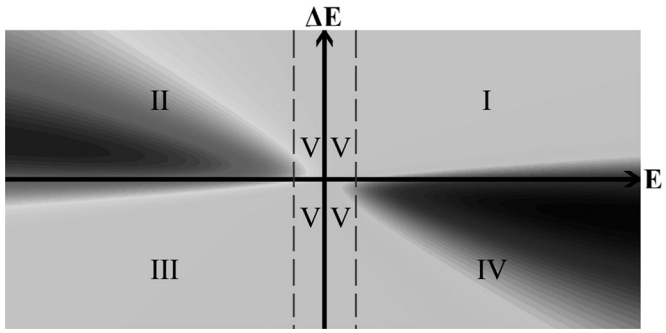

Fig. 1. Sectioning E – ΔE plane.

$$T_{\mathrm{Delay}} = h(|\Delta D|) = a' \times \Delta D + b' \tag{5}$$

where a' and b' are constant values. This mechanism means that controller waits T_{Delay} seconds after applying ΔD.

B. Perturbation Step-Size Generator

The slope of P–V curve is zero at MPP. The methods such as incremental conductance (INC) [8] and fuzzy MPPT [16], [20] work based on this fact. This feature has been also exploited in this paper for tracking the MPP along with the definition of an efficient function for generating the size of duty cycle perturbation. In order to explain how to design this function, the study of E and ΔE variation during all conditions and the expected behavior of the controller can be helpful.

1) Analyzing E–ΔE Plane: Considering the behavior of a PV cell and the perturbation step size that must be generated, the E–ΔE plane can be divided into 5 s as shown in Fig. 1. The black, dark gray, and light gray colors indicate the positive, negative, and zero perturbation step sizes that must be generated. Among these sections three main operational areas can be identified.

1) Zero-error (ZE) area: This area, which lies between two dashed lines, has been indicated by a "V" sign in Fig. 1 and represents an area with close proximity to MPP. The necessary condition of reaching MPP is satisfaction of $E = dP/dV = 0$ condition, but since a large jump in irradiance can cause this condition, the change of error or ΔE may vary significantly. Therefore, the ZE area is defined by a narrow strip along the ΔE axis and the origin neighborhood. In this area, the function should not change the operating point significantly, because in the next step, the error will remain constant, ΔE tends to zero, and afterward, the operating point returns to origin.
2) False-error (FE) area: This area includes two segments, which are indicated by "I" and "III" in Fig. 1. The points inside this area have large E and ΔE with the same sign. When the PV system operates in this area, the measured error and the change of error are not valid and reliable. In order to illustrate this issue, an example can be helpful. First, an operating point is assumed at left side of MPP. In this situation, the sign of E is positive. Afterward, an abrupt upward irradiance change occurs, causing the

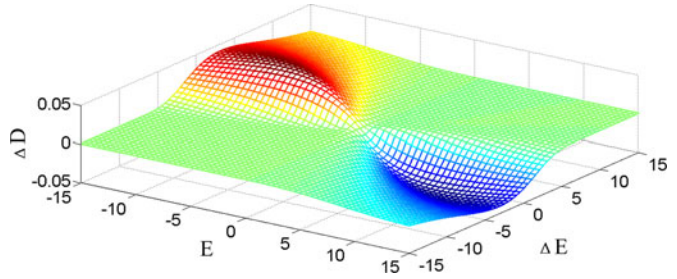

Fig. 2. Proposed function for generating duty cycle step sizes.

operating point to move to a new operating point on a new curve but the sign of E still remains unchanged while its amplitude becomes very large. In this case, both E and ΔE have the positive signs and large amplitudes. Therefore, in this area, it is unnecessary to apply large changes on duty cycle.

3) Valid-error (VE) area: This area comprises two subareas of "II" and "IV" in Fig. 1. The E and ΔE have opposite signs in these areas. The first segment is positive-error (PE) area (dark gray color) and has been marked with "IV." This area represents operating points that lie on the left side of MPP. When the system operates in this region, the terminal voltage of panel is less than MPP, and in order to move toward MPP, the voltage should be increased. Considering a boost converter, the duty cycle of converter should be decreased. Hence, the expected function in this area should generate a negative perturbation step size. The second segment is negative-error (NE) area (black color) marked with "II." This area represents the points that lie on the right side of MPP and have a negative slope (E) on P–V curve. When the PV system operates in this area, the output voltage of panel is larger than voltage of MPP. Therefore, the desired function should generate a positive step size.

2) Proposed Function: The expected function responsible for generating perturbation step size should exhibit a behavior in accordance with aforementioned features in each area. In addition, the function should result in a fast dynamic response, low oscillation in steady state, and robustness against large and fast changes in environment and load condition. The function proposed and investigated in this research has been formed by multiplication of a two-dimensional Gaussian function [21] and Arctangent function. Fig. 2 shows the behavior of this function in $E-\Delta E$ plane

$$\Delta D = f(E,\Delta E) = -1.4312 \times \Delta D_{\max} \times \tan^{-1}\left(\frac{E-\Delta E}{\gamma}\right) \times e^{\left(-\left(a(E-\alpha)^2+2b(\Delta E-\beta)(E-\alpha)+c(\Delta E-\beta)^2\right)\right)} \quad (6)$$

where $\Delta D_{\max}$ is the maximum allowable step size of duty cycle and γ is a constant. The coefficients of a, b, and c are obtained using the following formulas and values: (These coefficients have been determined based on trial and error method, but in general this can be done by using any optimization algorithm while considering performance indexes as objectives of optimization)

$$\theta = \frac{\pi}{10}, \quad \alpha = 0, \quad \beta = 0, \quad \gamma = 5, \quad \Delta D_{\max} = 0.05,$$
$$\sigma_E = 40 \quad \sigma_{\Delta E} = \sigma_{\Delta E0} + k\,|E-\Delta E|\,, \quad \sigma_{\Delta E0} = 0.5,$$
$$k = 0.25$$

$$a = \frac{\cos^2\theta}{2\sigma_E^2} + \frac{\sin^2\theta}{2(\sigma_{\Delta E0}+k\,|E-\Delta E|)^2} \quad (7)$$

$$b = -\frac{\sin 2\theta}{4\sigma_E^2} + \frac{\sin 2\theta}{4(\sigma_{\Delta E0}+k\,|E-\Delta E|)^2} \quad (8)$$

$$c = \frac{\sin^2\theta}{2\sigma_E^2} + \frac{\cos^2\theta}{2(\sigma_{\Delta E0}+k\,|E-\Delta E|)^2}. \quad (9)$$

In this part, the reasons of selecting the proposed function are explained. Using Arctangent operator guarantees that the step size will be always within preset bounds. Furthermore, it is an odd function which can generate correct sign in case of being in VE area. It is also a smooth function and most of the programming languages have the predefined library of this function. So, the function and consequently MPPT algorithm can be easily implemented in low cost digital controllers. The γ value in this function can expand or condense the Arctangent graph in the plane. So, it can speed up/down the variation of perturbation size and, consequently, the dynamic response of MPPT. Furthermore, proper selection of γ can improve the steady-state performance by limiting the oscillations around MPP. Another important feature that must be reflected in behavior of the proposed function is handling the false error situation. The Gaussian function has been used to damp the amplitude of step size in case of FE occurrence. When a large change occurs and E or ΔE gets large, the output of Gaussian function will get small in order to avoid large changes in duty cycle. The θ parameter has a significant influence on dynamic performance of algorithm by guaranteeing correct operation in FE area. In fact, this parameter rotates the FE and VE areas and determines the boundaries between these areas. Consequently, it can affect the correct dynamic performance of the system. The other important parameters are $\sigma_{\Delta E0}$, $\sigma_{\Delta E}$, and K, which determine the spread of the VE area in $E-\Delta E$ plane.

3) Generality of Method: The typical values of parameters selected in this study can be used for any panel. This advantage has been achieved by using scaled currents and voltages (short-circuit current and open-circuit voltage of panel in standard test condition (STC) are used for scaling). This causes E and ΔE to remain in a relatively fixed range. It has been tested on models of some PV panels. Test results showed that the differences between scaled curves are negligible. Furthermore, in selection of parameters, a soft boundary has been considered between areas for increasing the system robustness against small noises.

It must be noted that any function that is able to behave similar to proposed function can be used in this algorithm.

TABLE I
ELECTRICAL PARAMETERS OF PV CELL

Voltage at MPP	$V_{\mathrm{MPP}} = 23.1$ V
Current at MPP	$I_{\mathrm{MPP}} = 2.5$ A
Open-circuit voltage	$V_{\mathrm{oc}} = 30$ v
Short-circuit current	$I_{\mathrm{sc}} = 2.66$ A
Temperature coefficient of I_{sc}	0.024% °C^{-1}
Temperature coefficient of V_{oc}	−0.356% °C^{-1}

TABLE II
PARAMETERS OF ALGORITHMS

Method	Step Size (%)	Delay Time
GAF-VPF	0.1–5	$a = 0.136$, $b = 0.005$
Variable step-size INC	0.1–5	0.005 s
LCASF	0.1–5	$a = 0.136$, $b = 0.005$
Fuzzy	0.1–5	0.005 s

In addition, the proposed function provided in (6) performs correctly even in case of buck and buck–boost converters. So, it is independent of converter topology, which, in turn, makes it flexible for various situations.

III. SIMULATION

In order to assess the performance of proposed method, a 60-W PV panel has been simulated in MATLAB/Simulink. The electrical parameters of panel have been provided in Table I. The converter is a conventional boost regulator with a single MOSFET. In addition, variable step-size INC (VSSINC) [6], LCASF [15], and fuzzy [16] MPPT methods have been simulated for comparison among methods. Although, there are so many MPPT methods proposed in researches, this paper only deals with methods that only require current and voltage measurement. The details of implementing these methods have not been provided here for sake of brevity and only the main parameters of algorithms have been listed in Table II. The test scenarios comprise analyzing the performance and behavior of method during start-up, steady-state, and dynamic tests. Furthermore, the robustness of method to parameter changes has been investigated.

A. Startup Test

One of the proper tests for verifying the performance of MPPT algorithms is the start-up test. In this test, the system starts its operation with initial duty cycle of 10% in STC, and tracking behavior of the algorithm toward MPP is analyzed. In addition to GAF with variable perturbation frequency (GAF-VPF), GAF with fixed perturbation frequency (GAF-FPF) was used to do the test. Fig. 3 presents the output power of PV in case of startup test for a battery load. This figure shows that the algorithm performs well even in case of FPF, but the tracking speed has been reduced significantly in comparison with VPF.

The other performance index of MPPT algorithms is the transient rise time that is the time it takes the algorithm to reach 90% of the instantaneous maximum power in STC [22]. The

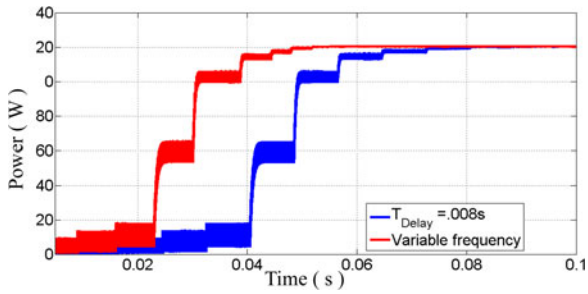

Fig. 3. Output power of PV for battery load in the start-up test.

TABLE III
RISE TIME OF METHODS IN MILLISECONDS

Method \ Load Type	Resistive load	Battery Load
GAF-VPF	85	46
GAF-FPF	116	78
Variable step-size INC	195	86
LCASF	146	72
Fuzzy	178	93

results have been provided in Table III. As the figures of table reflect, the proposed method performs better than other methods in term of transient rise time, i.e., time on the order of 46 ms to reach the MPP from initial state.

B. Steady-State Behavior

The steady-state performance of system has been investigated by computing the TF as follows [22]:

$$\eta_{\mathrm{MPPT}}(t) = \frac{\int_0^t P_{\mathrm{actual}}(\tau)\, d(\tau)}{\int_0^t P_{\mathrm{max}}(\tau)\, d(\tau)} \tag{10}$$

where P_{actual} is the measured output power, P_{max} is the expected or theoretical maximum power, and t indicates the duration of integration. The time interval of integration was considered 0.5 s in simulations. Additionally, presence of noise in measurements is an inevitable fact in all electrical systems. So, the steady-state performance of methods should also be analyzed in presence of noise. MPPT methods are differently affected by noise. In [23] and [24], a comprehensive study has been done on effects of noise on some MPPT techniques. In this study, random noises with maximum amplitude of $\pm 2\%$ of the main signals were added to voltage and current measurements and the TF of algorithms were computed. The same test was done for LCASF algorithm but only by applying the noise on current measurement. Table IV gives the results of computing TF in STC for a 40-Ω resistive load and considering both ideal and noisy measurement. As the figures in the table reveal, the efficiency of GAF-VPF has been less affected by noise measurement. The reason of this behavior lies in the fact that GAF-VPF can identify FE in case of a noisy voltage measurement producing large E. In addition, since there is no "if statement" in the proposed algorithm, it is less susceptible to get lost in algorithm conditional statements because of noise or error in measurements.

TABLE IV
PERFORMANCE OF METHODS IN STEADY STATE

Methods	TF in percent (for STC)		
	Noisy	Without Noise	Efficiency Loss
GAF-VPF	93.65	97.80	4.15
Variable step-size INC	90.24	97.32	7.08
Fuzzy	89.23	96.50	7.27
LCASF	90.10	96.60	6.50

Consequently, the cost of filter would be decreased while digital filtering can be easily exploited in microcontroller.

C. Dynamic Tests

In this section, the dynamic performance of proposed method has been investigated in comparison with other methods from different aspects including set-point tracking (step irradiance change and frequent ramp irradiance changes) and disturbance rejection (change in resistive load).

1) Step Irradiance Change: In this test, the irradiance changes at $t = 0.5$ s from 1000 to 300 W/m^2 and returns to 1000 at $t = 1.5$ s. It must be noted that the algorithm should be able to track the MPP both in step-up and step-down irradiance changes. Some methods move toward a wrong direction in case of step-down irradiance change. The results of simulation are presented in Fig. 4(a)–(d). These graphs show the variations of PV output power and corresponding duty cycle in response to mentioned changes. As it is clear from these graphs, VSSINC and LCASF loose the correct path. Moreover, in variable step size method, this wrong direction has been carried out by a large step size. The reason of these behaviors is inability of methods in distinguishing an FE. This wrong temporary maloperation has been addressed in [4] and [6]. When the irradiance changes, the duty cycle of MPP does not change considerably, but these methods change the duty cycle with a large step and cause the system to get far from MPP. Finally, they will return to MPP but after some additional steps. Fig. 4(a) and (b) clearly shows this issue. This maloperation leads to reduction in efficiency of controllers as the changes in irradiance occur frequently during a day. In contrast, fuzzy MPPT and proposed method do not suffer from this defect, because they are able to distinguish between false and valid errors. It must be noted that although the fuzzy MPPT also exhibits a good dynamic performance, it requires complicated considerations during its design. This complexity has led to utilization of metaheuristic methods for tuning the controller parameters in [16] and [25].

2) Frequent Ramp Irradiance Changes: In order to assess the dynamic performance of methods based on a numerical measure, a dynamic TF (DTF) was proposed and calculated using (10) and by applying a specific irradiance pattern. This pattern includes six upward and downward changes with different slopes and lasts for 25 s as shown in Fig. 5. The test also was carried out for two different cases of 50 Ω resistive load and a 40 V battery with internal resistance of 0.1 Ω. The computed DTFs have been provided in Table V. As explained before and

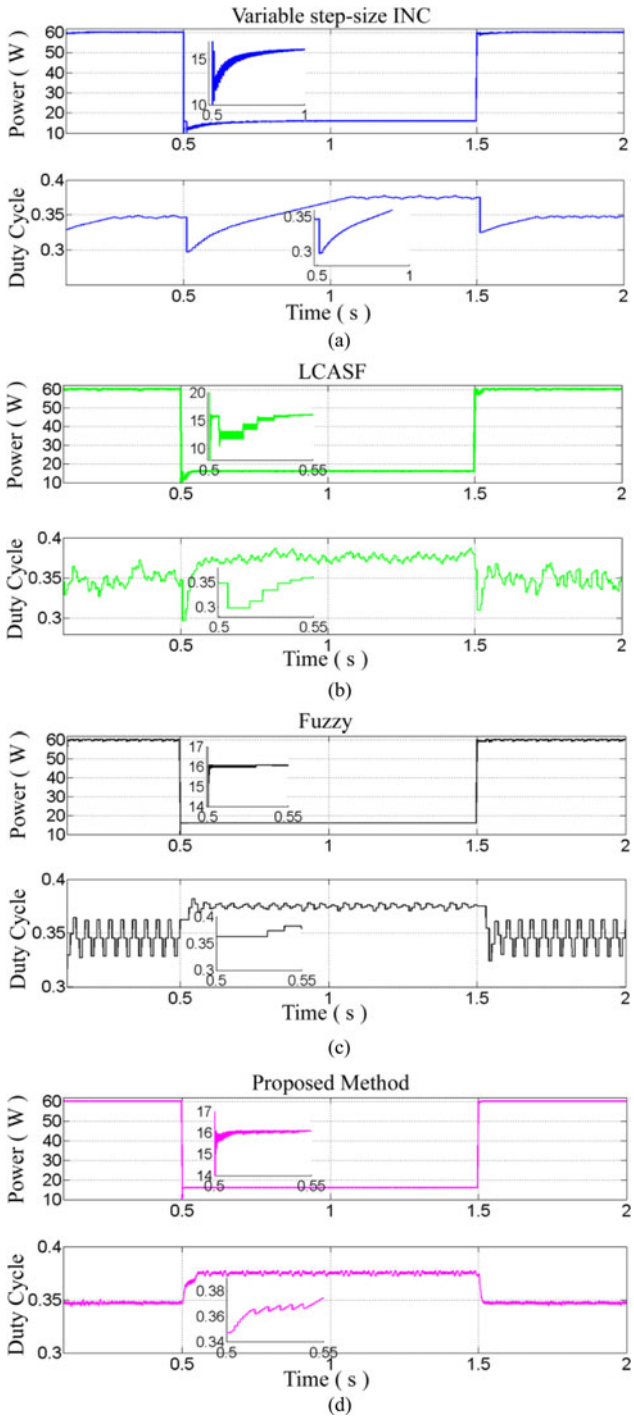

Fig. 4. Output power and duty cycle in step irradiance change for: (a) VSSINC, (b) LCASF method, (c) fuzzy method, and (d) proposed method.

figures of table show, the proposed method performs better than other methods in response to these irradiance changes. Its dynamic performance is also less sensitive to load conditions. The superiority of method in this test relies on proper definition of proposed function.

3) Disturbance Rejection (Change in Resistive Load): In this test, the change in load has been considered as a disturbance to the system, and the performance of algorithms was analyzed. A

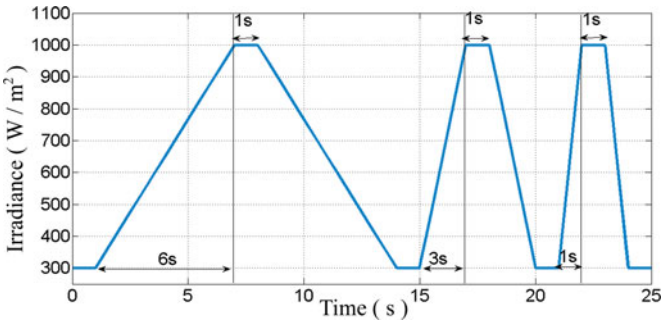

Fig. 5. Graph of irradiance pattern for evaluating dynamic performance.

TABLE V
DYNAMIC TF (%)

Method \ Load Type	Resistive load	Battery Load
GAF-VPF	97.58	97.65
GAF-FPF	96.63	96.72
Variable step-size INC	93.63	95.03
LCASF	95.62	96.51
Fuzzy	94.19	96.36

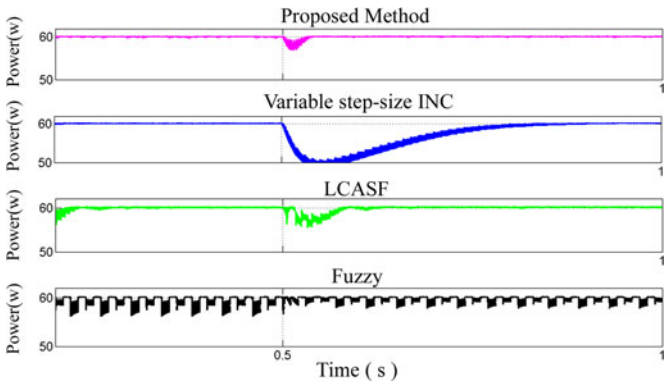

Fig. 6. Response of algorithms to load change.

60 Ω resistive load is connected to output terminal of converter and at $t = 0.5$ s, its resistance reduces to 40 Ω. The results have been depicted in Fig. 6. Evidently, it is apparent that the proposed method is able to remove the disturbance effect efficiently while VSSINC and LCASF methods exhibit poor performances because of their inability in recognizing false errors. Moreover, the Fuzzy method oscillates around MPP. The fuzzy method is not only very susceptible to become oscillatory in case of disturbance but also very hard to design. In fact, its parameters and membership functions should be tuned for any change in operating conditions.

4) Robustness with Respect to Parameters of Controller: Finally, the algorithm was tested against some changes in controller parameters. Although, the proposed controller should be implemented digitally and the parameters set in the digital controller do not change over the time, analyzing the performance of method with respect to these changes can be helpful for identifying the robustness and sensitivity of method with respect to design parameters. Therefore, $\gamma, \theta, \sigma_{\Delta E0}$, and K were changed and the performance of algorithm was tested. Table VI briefly explains the effect of each parameter on the performance and behavior of GAF-VPF method. Results showed that the algorithm is robust with respect to these changes. The algorithm was only somehow sensitive with respect to large changes in θ value because of its effect on definition of FE area. In addition, a very large change in γ makes the controller oscillatory around MPP and consequently decreases the steady-state performance. So, the proposed method is quite simple to design. Also, it does not require exact tuning of so many parameters like Fuzzy in which tuning of parameters is a hard and time-consuming task. Fig. 7(a)–(d) shows the response of proposed method to very large changes of, $\gamma, \theta, \sigma_{\Delta E0}$, and K.

TABLE VI
EFFECT OF PARAMETERS ON GAF-VPF METHOD

Parameter	Effect
γ	Improves the steady-state performance by decreasing the oscillations around MPP
θ	Improves the dynamic performance by guaranteeing correct operation in FE area
$\sigma_{\Delta E0}$	Improves the steady-state performance around MPP
K	Indicates the covering width of VE area

The last issue that must be noted about performance of MPPT controller is the shading phenomena. The algorithms usually perform well in areas with uniform environmental conditions but in case of shading, they must be updated in order to track the global MPPT instead of local MPPT. This update can be done by adding a first stage before applying the main algorithm [1], [26]. The issue of partial shading has been addressed in many recent researches such as [27], [28] and analyzing its effects is beyond the scope of this paper.

IV. EXPERIMENTAL RESULTS

A laboratory prototype was developed to test the proposed control method experimentally as shown in Fig. 8. The electrical scheme of the boost converter and all parameters and nominal operating conditions of system are presented in Table VII. The PV panel was a 53 W polycrystalline solar panel by Siemens selected different from the panel tested in simulations to show the generality of method for any panel type. As shown inFig. 9, the converter's output terminals was connected to the series connection of two 12-V lead acid battery paralleled by a 40-Ω resistor. A 32-bit 150-MHz digital signal controller TMS320F28335 from Texas Instruments was used as the main controller. The proposed GAF-VPF technique was practically tested using the same setup as mentioned in simulations and compared with VSSINC method.

Fig. 10(a) and (b) shows the performance of GAF-VPF and VSSINC in case of the start-up test. It is evident from these graphs that the proposed method outperforms the VSSINC in terms of rise time and steady-state oscillations around MPP. The rise time for GAF-VPF was 90 ms while it was 150 ms for VSSINC method. These results are relatively in accordance with simulation results and prove the fast response of GAF-VPF.

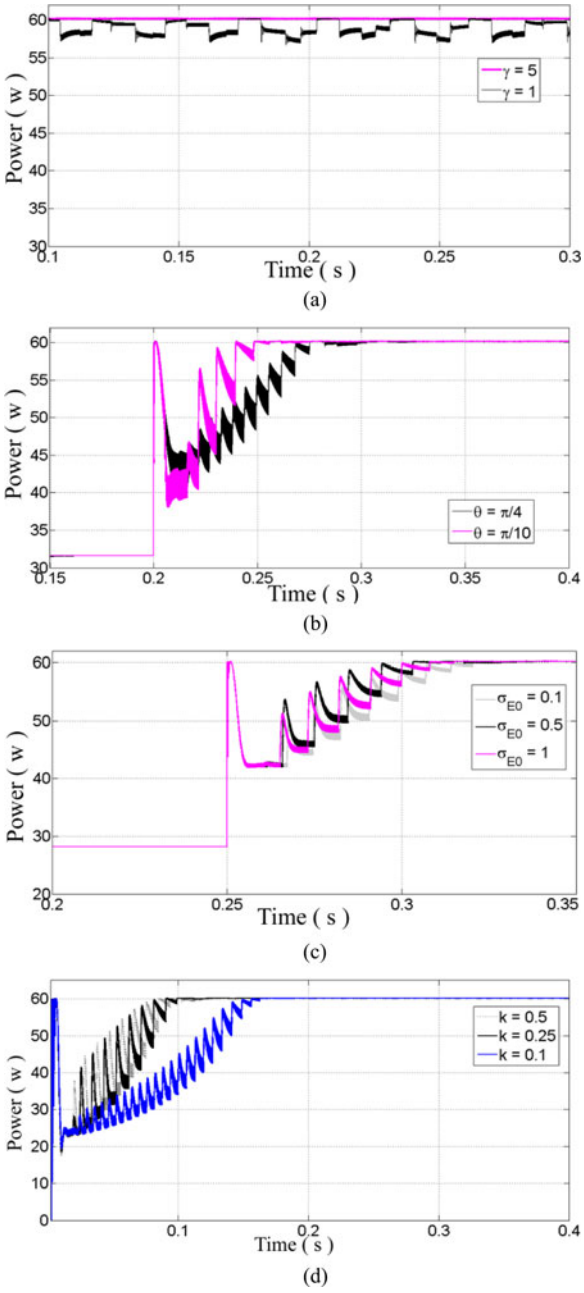

Fig. 7. Response of GAF-VPF algorithm to changes in (a)γ, (b) θ, (c) $\sigma_{\Delta E0}$, and (d) k.

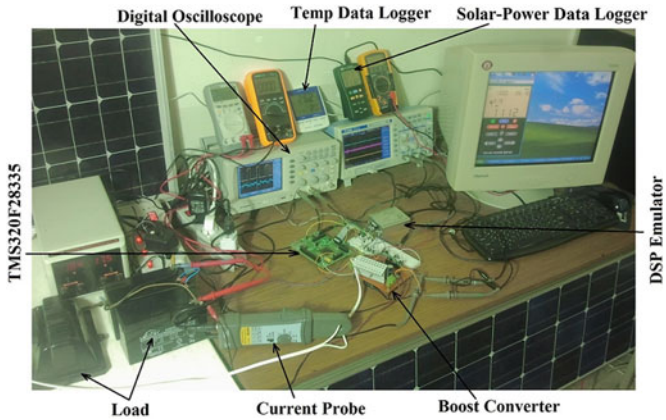

Fig. 8. Laboratory prototype.

TABLE VII
PARAMETERS AND NOMINAL OPERATING CONDITIONS FOR THE LABORATORY PROTOTYPE

PV Array	Values at STC
Short-circuit current	3.35 A
Open-circuit voltage	21.7 V
MPP current	3.05 A
MPP voltage	17.4 V
Temp. coefficient of I_{sc}	0.065 % °C^{-1}
Temp. coefficient of V_{oc}	−0.160 mV/°C
Boost parameters	Nominal values
Input capacitance C_{in}	100 μF
Output capacitance C_{out}	1000 μF
Inductance L	1000 μH
Operating conditions	Nominal values
Nominal switching frequency	20 kHz
Average output voltage	24 V

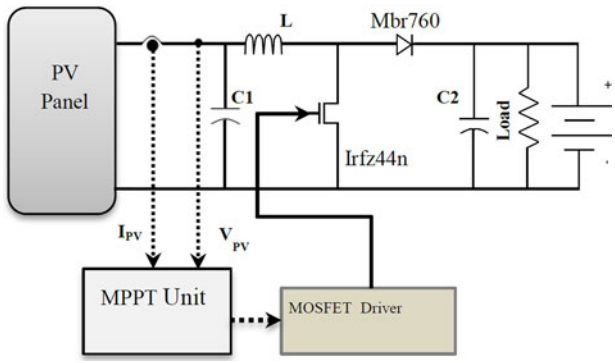

Fig. 9. Electrical scheme of the system under test.

In addition, the algorithm was able to track the correct MPP efficiently and with fewer oscillations in comparison with VSSINC method. These oscillations can be seen clearly in voltage waveforms. Although, Fig. 10(a) and (b) shows good performance of the proposed technique at steady-state and startup test, sudden irradiance change conditions also need to be addressed. Hence, the condition was emulated by using two identical PV panels connected in parallel and suddenly disconnecting one of them, thus reproducing a 50% sudden irradiance change.

Fig. 11(a) and (b) shows the behavior of two methods in response to mentioned irradiance change. It is evident that the proposed method leads to a better dynamic response. As it is clear from Fig. 11(b), the VSSINC method is unable to realize the occurrence of false error, so it has first generated a wrong step size for duty cycle and after a while it has modified its wrong decision.

Finally, the TF was computed for duration of 60 s in a sunny day. The resulted TF from experiments was 97% for GAF-VPF, while it was 96.8% in case of VSSINC method. A very small difference in TF of methods reveals the fact that the main contribution of the proposed MPPT method is its proper dynamic

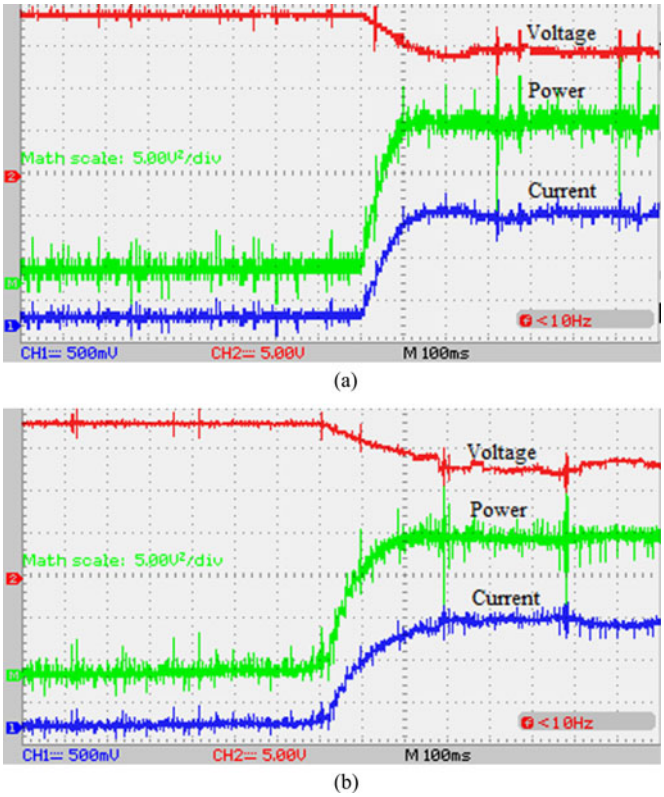

Fig. 10. PV panel output power in the start-up test and experimental results for (a) GAF-VPF and (b) VSSINC.

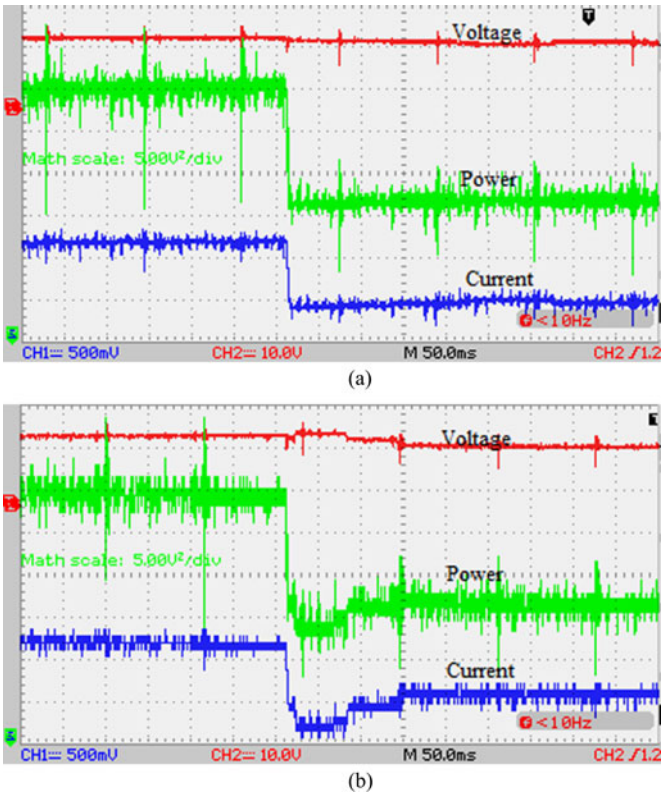

Fig. 11. PV panel output power, current, and voltage in the sudden insolation change and experimental results for (a) GAF-VPF and (b) VSSINC.

behavior and specially its correct operation in abrupt irradiance changes. This difference in TF may be increased when the TF is computed for a mobile solar application and for a longer time interval.

V. Conclusion

In this paper, a new MPPT algorithm named the GAF method was proposed. The method is based on introducing a complex function formed by multiplying a two-dimensional Gaussian function with an Arctangent function. This function is used for generating an adaptive perturbation size. In addition, variable perturbation frequency has been utilized for computing the time of applying the next duty cycle. Simulation results and experimental measurements confirm the attractiveness and superiority of the proposed method with respect to some well-known MPPT methods such as variable step-size incremental conductance, LCASF, and fuzzy method. The algorithm behaves robustly in case of load variation and measurement noise. The other advantage of proposed method is its simplicity of design. It does not require exact tuning of so many parameters. The only system-dependent constants required for controller setup are open-circuit voltage and short-circuit current and standard condition. Although, the computational cost of proposed method is higher than methods like P&O and incremental conductance, it can be easily implemented in low cost microcontrollers. Overall, these features make it well-suited for tracking uncommonly fast irradiance variations like mobile solar applications.

References

[1] M. A. G. de Brito, L. Galotto, Jr., L. P. Sampaio, G. de Azevedo e Melo, and C. A. Canesin, "Evaluation of the main MPPT techniques for photovoltaic applications," *IEEE Trans. Ind. Electron.*, vol. 60, no. 3, pp. 1156–1167, Mar. 2013.

[2] C. Hua, J. Lin, and C. Shen, "Implementation of a DSP-controlled photovoltaic system with peak power tracking," *IEEE Trans. Ind. Electron.*, vol. 45, no. 1, pp. 99–107, Feb. 1998.

[3] A. R. Reisi, M. H. Moradi, and S. Jamasb, "Classification and comparison of maximum power point tracking techniques for photovoltaic system: A review," *Renew. Sustainable Energy Rev.*, vol. 19, pp. 433–443, Mar. 2013.

[4] Q. Mei, M. Shan, L. Liu, and J. M. Guerrero, "A novel improved variable step size incremental-resistance MPPT method for PV systems," *IEEE Trans. Ind. Electron.*, vol. 58, no. 6, pp. 2427–2434, Jun. 2011.

[5] N. Femia, G. Petrone, G. Spagnuolo, and M. Vitelli, "Optimization of perturb and observe maximum power point tracking method," *IEEE Trans. Power Electron.*, vol. 20, no. 4, pp. 963–973, Jul. 2005.

[6] F. Liu, S. Duan, F. Liu, B. Liu, and Y. Kang, "A variable step size INC MPPT method for PV systems," *IEEE Trans. Ind. Electron.*, vol. 55, no. 7, pp. 2622–2628, Jul. 2008.

[7] A. K. Abdelsalam, A. M. Massoud, S. Ahmed, and P. N. Enjeti, "High-performance adaptive perturb and observe MPPT technique for photovoltaic-based microgrids," *IEEE Trans. Power Electron.*, vol. 26, no. 4, pp. 1010–1021, Apr. 2011.

[8] A. Safari and S. Mekhilef, "Simulation and hardware implementation of incremental conductance MPPT with direct control method using cuk converter," *IEEE Trans. Ind. Electron.*, vol. 58, no. 4, pp. 1154–1161, Apr. 2011.

[9] F. Liu, S. Duan, F. Liu, B. Liu, and Y. Kang, "A variable step size INC MPPT method for PV systems," *IEEE Trans. Ind. Electron.*, vol. 55, no. 7, pp. 2622–2628, Jul. 2008.

[10] S. L. Brunton, C. W. Rowley, S. R. Kulkarni, and C. Clarkson, "Maximum power point tracking for photovoltaic optimization using ripple-based extremum seeking control," *IEEE Trans. Power Electron.*, vol. 25, no. 10, pp. 2531–2540, Oct. 2010.

[11] M. H. Moradi, S. M. Reza Tousi, M. Nemati, N. Saadat Basir, and N. Shalavi, "A robust hybrid method for maximum power point tracking in photovoltaic systems," *Solar Energy*, vol. 94, pp. 266–276, Aug. 2013.
[12] R. Khanna, Q. Zhang, W. E. Stanchina, G. F. Reed, and Z. H. Mao, "Maximum power point tracking model reference adaptive control," *IEEE Trans. Power Electron.*, vol. 29, no. 3, pp. 1490–1499, Mar. 2014.
[13] H.-C. Chen and W.-J. Lin, "MPPT and voltage balancing control with sensing only inductor current for photovoltaic-fed, three-level, boost-type converters," *IEEE Trans. Power Electron.*, vol. 29, no. 1 , pp. 29–35, Jan. 2014.
[14] G.-C. Hsieh, H.-I. Hsieh, C.-Y. Tsai, and C.-H. Wang, "Photovoltaic power-increment-aided incremental-conductance MPPT with two-phased tracking," *IEEE Trans. Power Electron.*, vol. 28, no. 6, pp. 29–35, Jun. 2013.
[15] Y. Jiang, J. A. Abu Qahouq, and T. A. Haskew, "Adaptive step size with adaptive-perturbation-frequency digital MPPT controller for a single-sensor photovoltaic solar system," *IEEE Trans. Power Electron.*, vol. 28, no. 7, pp. 3195–3205, Jul. 2013.
[16] A. Messai, A. Mellit, A. Guessoum, and S. A Kalogirou "Maximum power point tracking using GA optimized fuzzy logic controller and its FPGA implementation," *Solar Energy*, vol. 85, no. 2, pp. 265–277, Feb. 2011.
[17] M. A. Elgendy, B. Zahawi, and D. J. Atkinson, "Assessment of perturb and observe MPPT algorithm implementation techniques for PV pumping applications," *IEEE Trans. Sustainable Energy*, vol. 3, no. 1, pp. 21–33, Jan. 2012.
[18] D. Shmilovitz, "Photovoltaic maximum power point tracking employing load parameters," in *Proc. IEEE Int. Symp. Ind. Electron.*, Jun. 2005, vol. 3, pp. 1037–1042.
[19] A. S. Kislovski and R. Redl, "Maximum power tracking using positive feedback," in *Proc. 25th Annu. IEEE Power Electron. Spec. Conf.*, Jun. 1994, pp. 1065–1068.
[20] R. Rahmani, M. Seyedmahmoudian, S. Mekhilef, and R. Yusof, "Implementation of fuzzy logic maximum power point tracking controller for photovoltaic system," *Amer. J. Appl. Sci.*, vol. 10, no. 3, pp. 209–218, 2013.
[21] N. Hagen and E. L. Dereniak, "Gaussian profile estimation in two dimensions," *Appl. Opt.*, vol. 47, pp. 6842–6851, 2008.
[22] S. L. Brunton, C. W. Rowley, S. R. Kulkarni, and C. Clarkson, "Maximum power point tracking for photovoltaic optimization using ripple-based extremum seeking control," *IEEE Trans. Power Electron.*, vol. 25, no. 10, pp. 2531–2540, Oct. 2010.
[23] A. M. Latham, R. Pilawa-Podgurski, K. M. Odame, and C. R. Sullivan, "Analysis and optimization of maximum power point tracking algorithms in the presence of noise," *IEEE Trans. Power Electron.*, vol. 28, no. 7, pp. 3479–3494, Jul. 2013.
[24] H. Al-Atrash, I. Batarseh, and K. Rustom, "Statistical modeling of DSP-based Hill-climbing MPPT algorithms in noisy environments," in *Proc. Appl. Power Electron. Conf. APEC 2005 (20th Annu. IEEE)*, Mar. 2005, vol. 3, pp. 1773–1777.
[25] C. S. Chin, P. Neelakantan, H. P. Yoong, and K. T. K. Teo, "Optimisation of fuzzy based maximum power Point tracking in pv system for rapidly Changing solar irradiance," *Trans. Solar Energy Planning*, vol. 2, pp. 130–137, 2011.
[26] R. Alonso, P. Ibanez, V. Martinez, E. Romen, and A. Sanz, "An innovative perturb, observe and check algorithm for partially shaded PV systems," in *Proc. 13th EPE*, 2009, pp. 1–8.
[27] P. Sharma and V. Agarwal, "Exact maximum power point tracking of grid-connected partially shaded PV source using current compensation concept," *IEEE Trans. Power Electron.*, vol. 29, no. 9, pp. 4684–4692, Sep. 2014.
[28] Y. Hu, W. Cao, J. Wu, B. Ji, and D. Holliday, "Thermography-based virtual MPPT scheme for improving PV energy efficiency under partial shading conditions," *IEEE Trans. Power Electron.*, vol. 29, no. 11, pp. 5667–5672, Nov. 2014.

S. M. Reza Tousi (M'13) received the B.Sc. degree in power electrical engineering from Sharif University of Technology, Tehran, Iran, in 1999, and the M.Sc. and Ph.D. degrees in electrical engineering from Amirkabir University of Technology (Tehran Poly-Techniques), Tehran, in 2002 and 2011, respectively.

Since January 2011, he has been collaborating with the Electrical Engineering Department, University of Bu-Ali Sina, Hamedan, Iran, where he is currently an Assistant Professor and the Director of Solar Electric Vehicle Laboratory. His current research interests include power electronics, renewable energies, photovoltaic systems, electric vehicles, and computational intelligence.

Mohammad Hassan Moradi (M'08) received the B.Sc. degree from Sharif University of Technology, Tehran, Iran, in 1991, the M.Sc. degree from Tarbiat Modares University, Tehran, in 1993, and the Ph.D. degree from Strathclyde University, Glasgow, U.K., in 2002.

He is currently a Lecturer in the Department of Electrical Engineering, University of Bu-Ali Sina, Hamedan, Iran. His current research interests include new and green energy, microgrid modeling and control, combined heat and power plant, supervisory control, and fuzzy control.

Nasser Saadat Basir received the B.Sc. and M.Sc. degrees in power electrical engineering from the University of Bu-Ali Sina, Hamedan, Iran, in 2012 and 2014, respectively. He is currently working toward the Ph.D. degree in power electrical engineering at Ferdowsi University, Mashahd, Iran.

His current research interests include photovoltaic systems, wind energy systems, and power electronics.

Milad Nemati was born in Hamedan, Iran. He received the B.Sc. and M.Sc. degrees in power electrical engineering from the University of Bu-Ali Sina, Hamedan, Iran, in 2012 and 2014 respectively.

He is currently collaborating with the Solar Electric Vehicle Laboratory, Department of Electrical Engineering, Bu-Ali Sina University. His current research interests include photovoltaic systems, electric vehicles, voltage control of microgrids, and power electronics.